Problems of confinement in QCD.

KHAIDUKOV Z.V

National Research Center Kurchatov Institute, ITEP
Moscow Institute of Physics and Technology.
07.25.2024

Motivation

We will discuss the recent development of the Field Correlator Method (FCM), with applications to the most interesting areas of QCD physics obtained in the lattice data and experiment. These areas include:
a) the theory of the colormagnetic confinement at all temperatures;
b) The theory of colormagnetic and colorelectric interactions and their applications to QCD thermodynamics also as for observable effects.

Field Cumulant method.

First steps

The aim is to find fundamental properties of the vacuum configurations which ensure confinement, and more technically, to introduce a formalism which enables one to describe long-range processes in terms of background-field vacuum correlators. At the present stage no proof of the proposed approach can be given, some assumptions can be however qualitatively checked against experimental data and conventional wisdom.

Field Cumulant method.

Main statements

We assume that gluon fields can be decomposed into the non-perturbative part and quantum fluctuations.

We assume that both non-perturbative gauge potentials and non-perturbative fields strength's are large in the QCD scale

All physical amplitudes and Green functions are obtained by averaging over background field configurations.

QCD vacuum correlation length is extremely small i.e we are dealing with stochastic vacuum

Field Cumulant method.

What's the price for that?

The area law in this model, Between colour charges!

$$< W(C) >= exp(-\sigma S_{min})$$
$$\sigma = \frac{1}{2}\int d^2 x D(x)(1 + O(FT_g^2))$$

D(x) is some function that we will describe below, $O(FT_g^2)$ is contribution of higher order cumulants. F is gluon field strength, T_g - vacuum correlation length.

Field Cumulant method. Some illustrations.

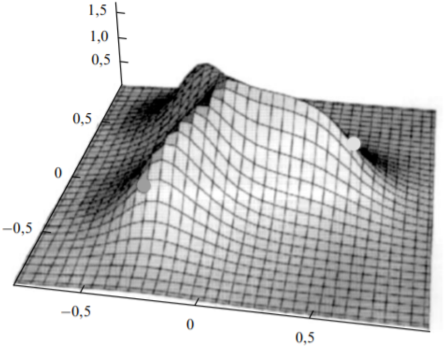

Рис. 15. Распределение поля $\mathcal{E}^{(\mathrm{B})}$ (80), (81) с учетом только вклада коррелятора D в плоскости кварков, образующих равносторонний треугольник со стороной 1 фм. Положения кварков показаны точками.

Figure: The baryon in the FCM picture.

Field Cumulant method.Some illustrations.

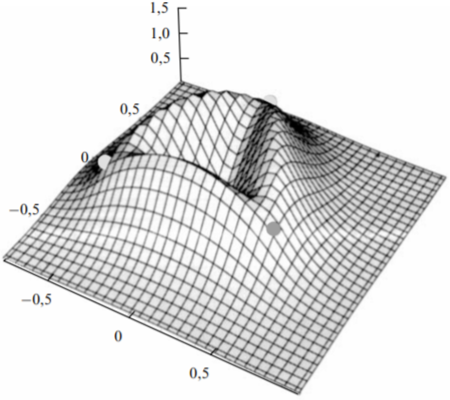

Рис. 18. Распределение поля $|\mathcal{E}_{\Delta}^{(G)}(\mathbf{x})|$ (82) треугольного глюбола в плоскости валентных глюонов, расстояние между которыми 1 фм. Положения валентных глюонов показаны точками.

Figure: The glueball in the FCM picture.

Field Cumulant method.Some illustrations.

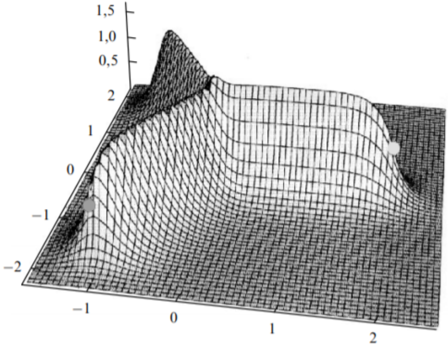

Рис. 16. Распределение поля $\mathcal{E}^{(B)}$ (80), (81) с учетом только вклада коррелятора D в плоскости кварков, образующих равносторонний треугольник со стороной 3,5 фм. Положения кварков показаны точками.

Figure: The baryon in the FCM picture.

Field Cumulant method.Some illustrations.

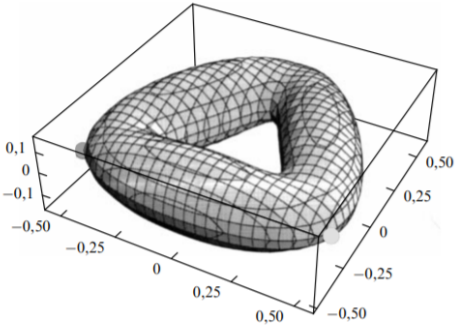

Рис. 19. Поверхность $|\mathcal{E}_{\Delta}^{(G)}(\mathbf{x})| = \sigma$ при расстоянии между валентными глюонами 1 фм. Положения валентных глюонов показаны точками.

Figure: The glueball in the FCM picture.

String tension important relations.

As a consequence of our assumption of very small correlation length an important role in FCM plays bilocal correlator (BC) of gluonic fields strength :

$$\frac{g^2}{N_c} < tr_f \Phi(y,x) F_{\mu\nu}(x) \Phi(x,y) F_{\lambda\rho}(y) > \equiv D_{\mu\nu,\lambda\rho}(x,y)$$

Symbol $<>$ means averaging over Yang-Mills action
$S = \frac{1}{4g^2} \int d^4x (F^a_{\mu\nu})$
$F^a_{\mu\nu} = \partial_\mu A_\nu - \partial_\nu A_\mu + g f^{abc} A^b_\mu A^c_\nu, a = 1..N_c^2 - 1$
$\Phi(x,y) = Pexp(i \int_y^x A_\mu dz^\mu), \mu = 1..4$ is the Wilson line in fundamental representation.

Strings tension main relations.

As for BC:

$$\frac{g^2}{N_c} < tr_f \Phi(y,x) F_{\mu\nu}(x) \Phi(x,y) F_{\lambda\rho}(y) > \equiv D_{\mu\nu,\lambda\rho}(x,y)$$

We can write BC as follows:

$$D_{\mu\nu,\lambda\rho}(x,y) = (\delta_{\mu\lambda}\delta_{\nu\rho} - \delta_{\mu\rho}\delta_{\nu\lambda}) D(x-y) + \\ + \frac{1}{2}(\frac{\partial}{\partial x_\mu}(x-y)_\lambda \delta_{\nu\rho} + perm.)) D_1(x-y)$$

$D(x-y), D_1(x-y)$ - are scalar functions. We also can add index E or H in D,D1 , because colormagnetic and colour electric contributions separates in sense $<< EH >>= 0$.

Strings tension main relations.

Functions $D^{E,H}(x)$, $D_1^{E,H}(x)$ define all confining QCD dynamics and in particular the string tensions:

$$\sigma_E = 1/2 \int (d^2 z)_{i4} D^E(z), \sigma_H = 1/2 \int (d^2 z)_{ik} D^H(z)$$

If we define a dependency of $D^{E/H}(z)$ with temperature we will obtain string tension ($\sigma_{E/H}$) behaviour.

Strings tension main relations.

The most interesting fact is that at $T > 0$ $\sigma_E(T)$ and $\sigma_H(T) = \sigma_s(T)$ behave differently. Namely: $\sigma_E(T)$ displays a spectacular drop before $T = T_c$ and disappears above $T = T_c$, while in contrast to that $\sigma_s(T)$ grows almost quadratically at large T

As a consequence tremendous differences in colourmagnetic and colourelectric condensates behaviours.

Gluelump and bilocal correlator of gluonic field strength.

We need to find a connection between $D(x)$ and so called gluelump Green's function.

For this purpose we rewrite the expression for BC in the form:

$$\frac{g^2}{N_c} < tr_f \Phi(y,x) F_{\mu\nu}(x) \Phi(x,y) F_{\lambda\rho}(y) >=$$

$$= \frac{g^2}{N_c} tr_f < F^a_{\mu\nu}(x) [T^a \Phi(x,y) T^b \Phi(y,x] F_{\lambda\rho}(y) >$$

The integration in the last expression is performed along the straight line connecting the points x and y. Thus we obtain the following expression:

Gluelump and bilocal correlator of gluonic field strength.

Thus we obtain the following expression

$$2tr(T^a\Phi(x,y)T^b\Phi(y,x)) = \Phi^{ab}_{adj}(x,y),$$

and finally we have:

$$D_{\mu\nu,\lambda\rho}(x,y) = \frac{g^2}{2N_c^2} tr_{adj} < F^a_{\mu\nu}(x)\Phi^{ab}_{adj}(x,y)F^b_{\lambda\rho}(y) >$$

At the next step we need to find connection between BC and so called gluelump Green's functions .

Gluelump and bilocal correlator of gluonic field strength.

Expanding $F_{\mu\nu}$ into abelian (parentheses) and nonabelian parts:

$$F_{\mu\nu} = (\partial_\mu A_\nu - \partial_\nu A_\mu) - ig[A_\mu, A_\nu]$$

we can write BC as:

$$D_{\mu\nu,\lambda\rho}(x,y) = D^0_{\mu\nu,\lambda\rho}(x,y) + D^1_{\mu\nu,\lambda\rho}(x,y) + D^2_{\mu\nu,\lambda\rho}(x,y)$$

where the number at the top of the letter D means power minus two of coupling constant g.

Gluelump and bilocal correlator of gluonic field strength.

For $D^0(x,y)$ we obtain:

$$D^0_{\mu\nu,\lambda\rho}(x,y) = \frac{g^2}{2N_c^2}(\frac{\partial}{\partial x_\mu}\frac{\partial}{\partial y_\nu}G^{1g}(x,y) + perm.) + \Delta^0_{\mu\nu,\lambda\rho}$$

$\Delta^0_{\mu\nu,\lambda\rho}(x,y)$ contains contribution of higher field cumulants, which we systematically discard.

We obtained the expression for one-gluelump Green function:

$$G^{1g}_{\mu\nu}(x,y) =< tr_{adj}\hat{A}_\mu(x)\hat{\Phi}_{adj}(x,y)\hat{A}_\nu(y) >$$

Gluelump and bilocal correlator of gluonic field strength.

$$G^{1g}_{\mu\nu}(x,y) =< tr_{adj} \hat{A}_\mu(x) \hat{\Phi}_{adj}(x,y) \hat{A}_\nu(y) >$$

From the physical point of view this equation describes the gluon that is moving in the field of adjoint source. Interaction between two objects in the adjoint representation is leading to formation of the string that according to Casimir scaling law found in the framework of FCM.

Gluelump and bilocal correlator of gluonic field strength.

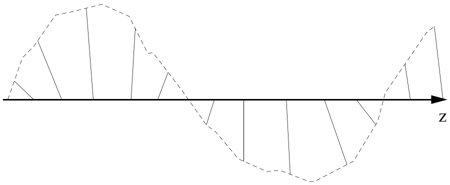

Figure: One-gluelump Green function.Bold straight line is trajectory of adjoint source that interacts with gluon (dashed line) through adjoint string).

Gluelump and bilocal correlator of gluonic field strength.

$D^2_{\mu\nu,\lambda\rho}(x,y)$ is of basic importance, since ensures confinement via D(x-y) and is expressed via two-gluon gluelump Green's function $G^{2g}(x,y)$.

The expression for $D^2_{\mu\nu,\lambda\rho}(x,y)$ reads as:

$$D^2_{\mu\nu,\lambda\rho}(x,y) = -\frac{g^4}{2N_c^2} < tr_{adj}([A_\mu(x), A_\nu(x)]\hat{\Phi}(x,y)[A_\lambda(y), A_\rho(y)]) >$$

Its immediately yields the following expression for D(x-y):

$$D(x-y) = \frac{g^4(N_c^2-1)}{2} G^{2gl}(x,y)$$

Gluelump and bilocal correlator of gluonic field strength.

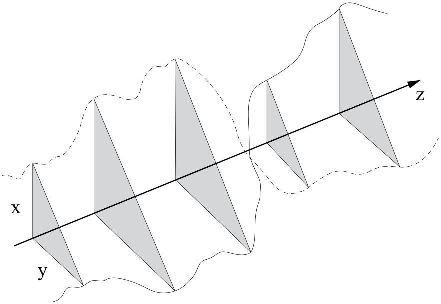

Figure: Two-gluelump Green function. Continuous and dashed lines are gluons trajectories. Bold straight line is trajectory of adjoint source. Shaded domain is x-y plane that is perpendicular to z axes. Sides of shaded triangle are fundamental strings.

Gluelump and bilocal correlator of gluonic field strength.

Two- gluelump Green's function at non-zero temperature reads as:

$$G^{2g}(x-y,T)=$$

$$=\int_0^\infty ds\int_0^\infty d\bar{s}\int D^w z_4 D^w \bar{z}_4 \int D^3 z D^3 \bar{z} exp(-S) < W(C_{z\bar{z}}) >$$

$$S=\frac{1}{4}\int_0^s d\tau(\frac{dz_\mu}{d\tau})^2+\frac{1}{4}\int_0^{\bar{s}} d\bar{\tau}(\frac{d\bar{z}_\mu}{d\bar{\tau}})^2$$

The Wilson loop $W(C_{z\bar{z}})$ is averaged over gluon fields along the paths z, $\bar{z}$ in the field of a static adjoint source with spatial coordinate $\vec{r}=(0,0,0)$ that moves along z-axis entirely. This procedure leads to formation of strings between gluons themselves and glouns and the source.

Gluelump and bilocal correlator of gluonic field strength.

One can calculate the part of the path integral in temporal direction:

$$J_4 \equiv \int (Dz_4)_{x_4 x_4} e^{-K_4} = \sum_{n=-\infty}^{+\infty} \frac{1}{2\sqrt{\pi s}} e^{-\frac{(n\beta)^2}{4s}}$$

$$J_{s,\bar{s}}(s, \bar{s}, T) = \frac{1}{4\pi\sqrt{s\bar{s}}} \vartheta_3(e^{-\frac{1}{4sT^2}}) \vartheta_3(e^{-\frac{1}{4\bar{s}T^2}})$$

Where we have used the relation:

$$\sum_{n=-\infty}^{+\infty} e^{-\frac{n^2}{4sT^2}} \equiv \vartheta_3(q), \quad q = e^{-\frac{1}{4sT^2}}$$

Gluelump and bilocal correlator of gluonic field strength.

$$G^{2g}(x-y,T)=\int_0^\infty ds\int_0^\infty d\bar{s}\int D^3zD^3\bar{z}exp(-S_{spatial})J_{s,\bar{s}}(s,\bar{s},T)$$

$S_{spatial}$ - is a rest part of the action without fourth component containing "spatial" Wilson factor.

Changing $s=\frac{t}{2\omega_1},\bar{s}=\frac{t}{2\omega_2}$,with third coordinate, as "Euclidean time

Gluelump and bilocal correlator of gluonic field strength.

Finally we obtain:

$$G^{2g}(t,T) = \frac{t}{8\pi}\int_0^\infty \frac{d\omega_1}{\omega_1^{3/2}}\int_0^\infty \frac{d\omega_2}{\omega_2^{3/2}}\int (D^2 z_1)_{xy}(D^2\bar{z}_2)_{xy}\cdot$$
$$\cdot e^{-\sum_{i=1,2}K_i(\omega_i)-Vt}\vartheta_3(e^{-\frac{\omega_1}{2tT^2}})\vartheta_3(e^{-\frac{\omega_2}{2tT^2}})$$

here label xy means xy-plane. For $K_i(\omega_i), i,j=1,2$:

$$K_i(\omega_i) = \int_0^t d\tau_E(\frac{\omega_i}{2}+\frac{\omega_i}{2}(\frac{dx_j}{d\tau_E})^2)$$

Gluelump and bilocal correlator of gluonic field strength.

The potential of interaction between gluons themselves and gluons with adjoint source reads as:

$$V(z, \bar{z}) = \sigma_f(|\vec{z}| + |\vec{\bar{z}}| + |\vec{z} - \vec{\bar{z}}|)$$

σ_f - is string tension in the fundamental representation.

So we have all ingredients to obtain the spatial string tension!

Spatial string tension.

After very complicated calcualtions we have:

$$\sigma_s(T) = \frac{g^4(T)(N_c^2-1)}{4} \int d^2 z z/(8\pi) \int d\omega_1 d\omega_2 (\omega_1\omega_2)^{-3/2}$$

$$\times \sum_{n=0,1,} |\psi_n(0,0)|^2 \exp(-M_n(\omega_1,\omega_2)z) f(\sqrt{z/2\omega_1}T) f(\sqrt{z/2\omega_2}T)$$

Running coupling

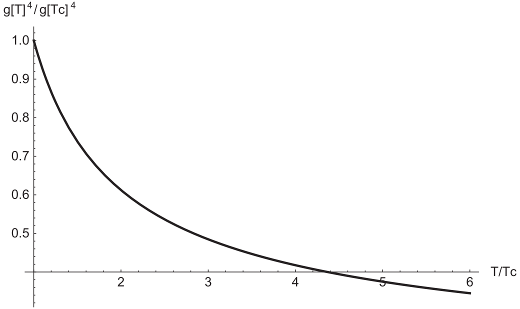

Figure: Behaviour of $\frac{g(T)^4}{g(T_c)^4}$ as a function of $\frac{T}{T_c}$.

At temperatures much lower than T_c there is a freezing of the running coupling.

Spatial string tension.

One can write $\sigma_s(T)$ after the averaging with respect to $\omega_{1,2}$ and z in the following form:

$$\sigma_s(T) = \mathrm{const} g^4(T) < f^2(\sqrt{z/(2\omega)T}) >$$

$$\sigma_s(T) = \mathrm{const} g^4(T) f^2(\sqrt{\overline{\mathrm{z}/2\omega}}T)$$

$$\sigma_s(T) = \mathrm{const} g^4(T) f^2(\overline{\mathrm{w}}T)$$

Lets test our arguments and try to find the value of $\overline{\mathrm{w}}$, that will describes the all lattice data for spatial string tension.

Running coupling

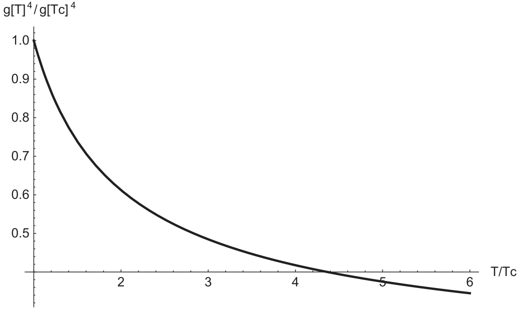

Figure: Behaviour of $\frac{g(T)^4}{g(T_c)^4}$ as a function of $\frac{T}{T_c}$.

At temperatures much lower than T_c there is a freezing of the running coupling.

General expression for the spatial string tension vs lattice data

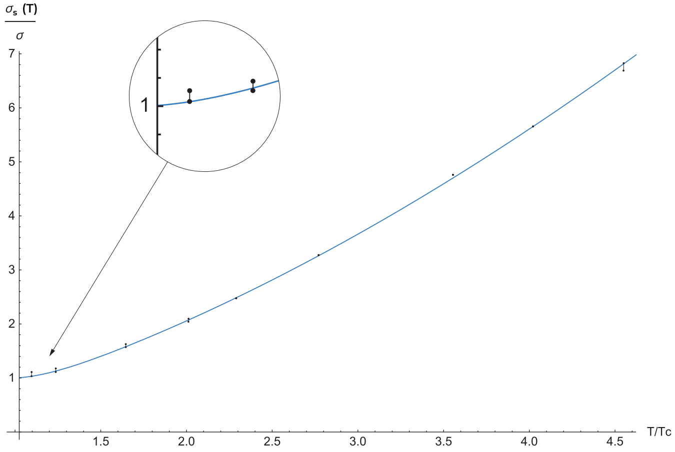

Figure: Spatial string tension $\sigma_s(T)/\sigma$ for SU(3) gauge theory as function of T/T_c. The lattice data with errors are from G. Boyd et al.,(Nucl. Phys. **B 469**), 419 (1996). T_c=270 MeV

Main results, And physical consequences.

We obtained color-magnetic string tension for various temperatures. Even at very high($5T_c$) temperatures the colour-magnetic string doesn't breaks

Non-perturbative dynamic and thermodynamic even at very big temperatures!Additional scale $\sqrt{\sigma_s}$ that is competed with T exists Non-perturbative Debye-mass that proportional to $\sqrt{\sigma(T)}$ emerges.Colour-magnetic condensate still growing with temperatures

Does colour-magnetic string never breaks?

Of course it breaks but at extremly high tempertures!

What's about physical applications.

At temperatures above deconfinement transition we can calculate thermodynamical potentials for QCD.It decomposes into two parts, for gluons we obtain:

$$P_{gl} = 2(N_c^2 - 1)\int_0^\infty \frac{ds}{s} \sum_{n=1,2..} G^n(s).$$

Here s is the proper time, and for $G^n(s)$ one can obtain:

$$G^n(s) = \int (Dz)^\omega_{on} exp(-K)\hat{tr}_a < W^a_\Sigma(C_n) >,$$

where $K = \frac{1}{4}\int_0^s d\tau \left(\frac{dz^\mu}{d\tau}\right)^2$, and $W^a_\Sigma(C_n)$ is the adjoint Wilson loop defined for the gluon path C_n, which has both temporal (i4) and spacial projections (ij), and $\hat{tr}_a$ is the normalized adjoint trace.

What's about physical applications.

When $T > T_c$ the correlation function between CE and CM fields is rather week:

$$<< E_i(x)\Phi(x,y)B_k(y)\Phi(y,x) >>\approx 0$$

and therefore, the expression for the Wilson loops is factorized:

$$< W_\Sigma^a(C_n) >= L_{adj}^{(n)}(T) < W_3 >$$

with $L_{adj}^{(n)} \approx L_{adj}^n$ for $T \leq 1$ GeV. One can integrate out the z_4 part of the path integral $(Dz)_{on}^\omega = (Dz_4)_{on}^\omega D^3 z$, with the result:

$$G^{(n)}(s) = G_4^{(n)}(s)G_3(s)$$

$$G_4^n(s) = \int (Dz_4)_{on}^\omega e^{-K} L_{adj}^{(n)} = \frac{1}{2\sqrt{4\pi s}} e^{-\frac{n^2}{4T^2 s}} L_{adj}^{(n)}$$

What's about physical applications.

The resulting gluon contribution is

$$P_{gl} = \frac{2(N_c^2 - 1)}{\sqrt{4\pi}} \int_0^\infty \frac{ds}{s^{3/2}} G_3(s) \sum_{n=0,1,2,\dots} e^{-\frac{n^2}{4T^2 s}} L_{adj}^n,$$

$$G_3(s) = \int (D^3 z)_{xx} e^{-K_{3d}} < \hat{tr}_a W_3^a >$$

The inclusion of colour-magnetic interaction leads to the generation of a non-perturbative Debye mass M_D for gluons and quarks. For gluons $M_{adj} \sim \sqrt{\sigma^H(T)}$, one can take it into account by an approximate expression for 3d Green function :

$$G_3(s) = \frac{1}{(4\pi s)^{3/2}} \sqrt{\frac{(M_{adj}^2)s}{sinh(M_{adj}^2)s}}$$

What's about physical applications.

In the non-interacting case i.e. $\sigma^H = 0$ and $L_{adj} = 1$ one obtains the ideal gas pressure:

$$P_{gl} = P_0 = \frac{(N_c^2 - 1)}{45}\pi^2 T^4$$

For quarks one can write the expression in the same form, but with the quark mass term $e^{-m_q^2 s}$:

$$P_f = \sum_{q=u,d,s} P_q$$

$$P_q = \frac{4N_c}{\sqrt{4\pi}} \int_0^\infty \frac{ds}{s^{3/2}} e^{-m_q^2 s} S_3(s) \sum_{n=1,2,\ldots} (-)^{n+1} e^{-\frac{n^2}{4T^2 s}} L_f^n$$

$$S_3(s) = \frac{1}{(4\pi s)^{3/2}} \sqrt{\frac{(M_f^2)s}{sinh(M_f^2)s}}, M_{adj}^2 = \frac{9}{4} M_f^2, L_n^f = (L_n^{adj})^{4/9}$$

And again in the case of massless non-interacting fermions one obtains:

$$P_f = N_c N_f \frac{7T^4}{180}$$

What's about physical applications.

The full pressure reads as:

$$P_{tot} = P_f + P_{gl}$$

To include the effects of the baryon chemical potential we should do the substitution:

$$L_f^n \to L_f^n cosh(\mu n/T)$$

And the expression for the pressure reads as:

$$P_f = \sum_{q=u,d,s} P_q$$

$$P_q = \frac{4N_c}{\sqrt{4\pi}} \int_0^\infty \frac{ds}{s^{3/2}} e^{-m_q^2 s} S_3(s) \sum_{n=1,2,\dots} (-)^{n+1} e^{-\frac{n^2}{4T^2 s}} L_f^n cosh(\frac{\mu n}{T})$$

$$S_3(s) = \frac{1}{(4\pi s)^{3/2}} \sqrt{\frac{(M_f^2)s}{sinh(M_f^2)s}}, M_{adj}^2 = \frac{9}{4} M_f^2, L_n^f = (L_n^{adj})^{4/9}$$

Comparing with the lattice data .

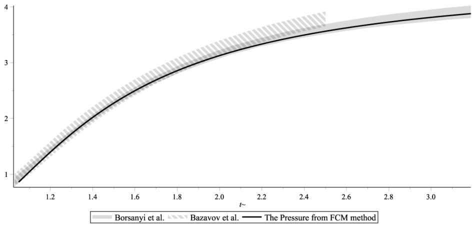

Figure: The pressure in comparison with the lattice data.

Comparing with the lattice data .

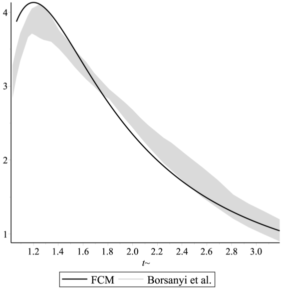

Figure: The anomaly in QGP as a function of T/T_c. The grey band is the lattice data of Borsanyi et al.

Comparing with the lattice data .

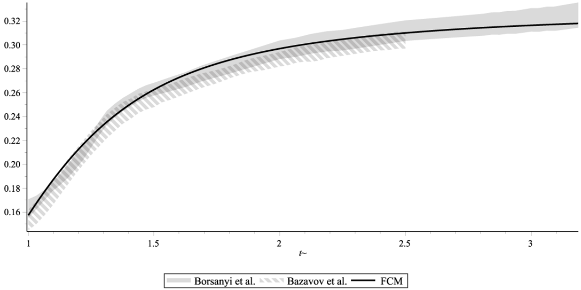

Figure: The speed of sound in QGP as a function of T/T_c. The grey band is the lattice data of Borsanyi et al. and the striped band is the lattice data from Bazavov et al.

Some remarks

CMC is an essential ingredient for QGP thermodynamics description.

Even at high enough temperatures strong interaction is still strong!

Some problems with Polyakov Line calculations.

Another way to test our assumptions!

Let's calculate some observables in QGP. For example currents!

In our technique we can calculate the axial current in thermodynamic equilibrium in uniform magnetic field in presence of chemical potential.So called chiral separation effect. In massless case the expression for the axial current reads as:

$$j^{5z} = \frac{e^2\mu}{2\pi^2} B^z$$

μ - chemical potential, B^z-magnetic field.

Another way to test our assumptions!

For obtaining the expression for the axial current we need to consider the lowest Landau level(LLL). In this case there is a relation:

$$j^{5z} = \pm(\psi_L^\dagger \psi_L + \psi_R^\dagger \psi_R) = j^0$$

and thus if we calculate charge density in the equilibrium on the LLL we obtain the axial current!

Another way to test our assumptions!

The value of the axial current:

$$< j^{5z} >_{T,V} = \mp N_c T \frac{e_q B_z}{2\pi} \frac{\partial}{\partial \mu} (\chi(\mu) + \chi(-\mu))$$

where:

$$\chi(\mu) = \int \frac{dp_z}{2\pi} ln(1 + exp(\frac{\tilde{\mu} - E^{\sigma}_{n_\perp}(B)}{T}))$$

$$\begin{aligned} \tilde{\mu} &= \mu - V_1(\infty, T)/2 \\ L &= exp(-V_1(\infty, T)/2) \end{aligned} \tag{1}$$

Thus we have all ingredients to obtain the value for CSE.

Another way to test our assumptions!

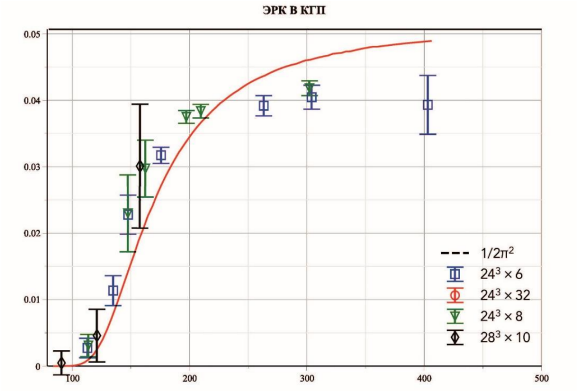

Figure: CSE coefficient in comparison with the lattice data.

THANK YOU FOR YOUR ATTENTION!